

<https://doi.org/10.3799/dqkx.2018.161>



海南荔枝沟中三叠世酸性火山岩年代学、 地球化学特征及其构造意义

苟琪钰, 钱 鑫*, 何慧莹, 张玉芝, 王岳军

广东省地球动力作用与地质灾害重点实验室, 中山大学地球科学与工程学院, 广东广州 510275

摘要:海南岛位于印支与华南陆块的交界地带, 构造演化复杂, 因此海南岛的拼合历史和构造属性一直备受争议。在海南岛三亚荔枝沟地区新识别出的酸性火山岩对于探讨海南岛早中生代的构造属性具有重要指示意义。LA-ICP-MS 锆石 U-Pb 定年结果显示该套酸性火山岩中流纹岩的成岩年龄为 241 ± 6 Ma (MSWD=0.9)。地球化学特征表明该套火山岩样品的 SiO_2 含量介于 72.34%~77.83%, 具较高的 Al_2O_3 (10.51%~13.53%)、 K_2O (2.85%~4.85%)、 Na_2O (1.75%~3.79%) 含量和 A/CNK 比值 (0.99~2.07), 为过铝质钙碱性酸性火山岩。样品稀土元素含量为 $\sum \text{REE} = 87 \times 10^{-6}$ ~ 177×10^{-6} , 富集轻稀土元素, 显示右倾弧型稀土元素配分模式, Eu 负异常明显。样品富集大离子亲石元素, 亏损高场强元素, $\epsilon_{\text{Nd}}(t)$ 变化于 -12.1 ~ -11.3 之间, 可被解释为变沉积物部分熔融后经历分离结晶作用的产物。区域对比研究表明该套酸性火山岩可与三江地区的金沙江—哀牢山—松马构造带的中三叠世岩浆岩进行类比, 应形成于印支与华南陆块汇聚的构造背景。

关键词:中三叠世; 酸性火山岩; 年代学; 地球化学; 碰撞后; 海南岛。

中图分类号:P595

文章编号: 1000-2383(2019)04-1357-14

收稿日期: 2018-04-03

Geochronological and Geochemical Constraints on Lizhigou Middle Triassic Felsic Volcanic Rocks in Hainan and Its Tectonic Implications

Gou Qiyu, Qian Xin*, He Huiying, Zhang Yuzhi, Wang Yuejun

Guangdong Provincial Key Laboratory of Geodynamics and Geohazards; School of Earth Science and Engineering,
Sun Yat-sen University, Guangzhou 510275, China

Abstract: Hainan Island, which is located between the Indochina and South China blocks, has undergone multiphased structural overprinting and complex tectonic evolution. However, the Late Paleozoic tectonic regime and amalgamation process of the South China with Indochina blocks are still controversial. The newly-identified felsic volcanic rocks in the Lizhigou area are important for understanding the Early Mesozoic tectonic evolution in Hainan. LA-ICP-MS zircon U-Pb dating results show that the representative rhyolite samples yield a weighted mean $^{206}\text{Pb}/^{238}\text{U}$ age of 241 ± 6 Ma (MSWD=0.9). These samples contain SiO_2 ranging from 72.34% to 77.83%, Al_2O_3 from 10.51% to 13.53%, K_2O from 2.85% to 4.85% and Na_2O from 1.75% to 3.79%. The A/CNK values range from 0.99 to 2.07. These samples have REE concentrations of 87×10^{-6} to 177×10^{-6} , and Eu/Eu^* of 0.49~0.65. They are characterized by subparallel right-sloping REE pattern and enrichment in LREEs and LILEs, and depletion in HFSEs, similar to those of arc volcanics. Their $\epsilon_{\text{Nd}}(t)$ values range from -12.1 to -11.3. These felsic volcanic rocks are the products of partial melting of metasediments with significant fractionation crystallization. In combination with other available data, it is inferred that the Lizhigou felsic volcanic rocks can be compared with the Middle-Late Triassic igneous

基金项目:国家自然科学基金项目(Nos.41830211, U1701641, 41702230); 广东省自然科学基金项目(No.2018B030312007); 中国科学技术部国家重点研发计划课题(No.2016YFC0600303)。

作者简介:苟琪钰(1995—), 女, 硕士研究生, 主要从事岩石大地构造研究. ORCID:0000-0001-9424-4329. E-mail:gouqy3@mail2.sysu.edu.cn

* 通讯作者:钱鑫, E-mail:qianx3@mail.sysu.edu.cn

引用格式:苟琪钰, 钱鑫, 何慧莹, 等, 2019. 海南荔枝沟中三叠世酸性火山岩年代学、地球化学特征及其构造意义. 地球科学, 44(4):1357~1370.

rocks along the Jinshajiang-Ailaoshan-Songma zone, and formed during the assemblage of the South China with Indochina blocks related to East Paleotethyan consumption.

Key words: Middle Triassic; felsic volcanic rock; geochronology; geochemistry; post-collisional setting; Hainan Island.

0 引言

东南亚地区保存了大量与古特提斯构造演化有关的岩浆岩及沉积记录,是研究古特提斯洋形成、演化、俯冲及消亡的天然实验室。海南岛地处太平洋、菲律宾板块和华南、印支陆块的交界部位,也是古太平洋构造域和古特提斯构造域的叠置区(图 1a),对于研究古特提斯洋的演化以及华南和印支陆块的聚合具有重要的意义(汪啸风等,1991; 李孙雄等,2005; 陈新跃等,2011,2014; 唐立梅等,2013; 温淑女等,2013; He *et al.*,2017,2018; Li *et al.*,2018)。

已有的研究表明海南岛北部地区存在石炭纪时期的岛弧及弧后盆地岩浆记录,并可以与金沙江—哀牢山—松马缝合带内相关的石炭纪岩浆岩进行对比(图 1a; Li *et al.*,2002,2018; He *et al.*,2017)。同时,岛内还广泛分布有大量的二叠纪—三叠纪岩浆岩(夏邦栋等,1990; 李孙雄等,2005; 谢才富等,2005; Li *et al.*,2006; Zhang *et al.*,2011; 陈新跃等,2011; 温淑女等,2013)。作为研究的热点,这些二叠纪—三叠纪岩浆岩的岩石成因及其构造背景众说纷纭,与之对应的二叠纪—三叠纪的构造演化史也未形成统一的定论。谢才富等(2005)在海南岛中部识别出了钾玄质侵入岩,并认为华南陆块与印支陆块的碰撞拼贴发生于 287~278 Ma,且华南陆块和印支陆块拼贴之间的缝合带可能是从越南松马地区,沿北部湾和云开大山北缘连接至武夷山地区。而其他学者结合海南岛早三叠世 NWW 向的构造变形(陈新跃等,2006; Zhang *et al.*,2011)和相关的三叠纪碱性岩、A 型花岗岩、高钾钙碱性花岗岩和镁铁质侵入岩等岩石组合,认为海南岛地区的 250 Ma 岩浆岩形成于同碰撞阶段,并在 240 Ma 之后进入到碰撞后阶段(谢才富等,2005; 唐立梅,2010; 唐立梅等,2013; 陈新跃等,2014)。

最近,笔者在海南岛三亚荔枝沟地区新识别出了一套酸性火山岩组合(包括流纹岩、凝灰岩、火山集块岩)。因此,本文选取该套酸性火山岩开展 LA-ICP-MS 钨石 U-Pb 年代学、全岩主、微量元素及 Sr-Nd 同位素研究,并结合区域地质资料研究该套酸性火山岩的岩石成因及其大地构造背景,进而为探讨古特提斯洋的构造演化提供重要依据。

1 区域地质背景与岩石学特征

海南岛地处中国东南部,以琼州海峡与华南大陆相隔。海南岛由北向南发育王五一文教、昌江—琼海、尖峰—吊罗、九所—陵水等多条近东西向的断裂(广东省地质矿产局,1988; 沈宝云等,2016);由西向东发育了戈枕、白沙等北东向断裂(夏邦栋等,1990,1991; 汪啸风等,1991)。海南岛主要出露古生界,其次为元古宇和中新生界(马大铨等,1998; 龙文国等,2002)。中元古代长城纪的抱板群和青白口纪的石碌群被认为是海南岛最古老的地层,主要出露于抱板、冲卒岭、昌江等地(广东省地质矿产局,1988; 汪啸风等,1991)。下古生界寒武系和奥陶系由一套浅变质页岩、砂岩、粉砂岩和板岩组成(夏邦栋等,1990; 汪啸风等,1991)。志留系为浅海相砂岩和一套过渡类型的碎屑岩、灰岩和板岩组合(胡宁等,2002; 龙文国等,2007)。分布于九所—陵水断裂以北的上古生界主要出露有泥盆系砂岩、石炭系板岩和变火山岩、下二叠统灰岩以及中二叠统砂岩(夏邦栋等,1990; 汪啸风等,1991; 胡宁等,2002; 龙文国等,2007)。中生界在岛内仅出露上三叠统碎屑岩沉积和白垩系砂岩(夏邦栋等,1990; 汪啸风等,1991)。岛内新生界发育完整,主要分布于海南岛北部(唐立梅,2010)。

由于强烈的岩浆活动,海南岛内岩浆岩广泛分布,占全岛面积 51% 的侵入岩可划分为海西、印支和燕山期花岗岩,其中海西与印支期花岗岩分布最广,其次为燕山晚期的花岗岩类。喷出岩以王五一文教断裂以北的新生代玄武岩为主(广东省地质矿产局,1988; 夏邦栋等,1990; 李献华等,2000; He *et al.*,2017; Li *et al.*,2018)。目前的资料表明:岛内二叠纪至三叠纪出现的侵入岩体包括五指山、育才、通什、道票岭、禄马、尖峰、袁水、立才、六连岭和万宁等多个超单元(广东省地质矿产局,1988; 温淑女等,2013)。

本次研究的酸性火山岩采自海南省九所—陵水断裂以南的三亚市荔枝沟地区(图 1b~1c),区内还分布有三叠纪和白垩纪花岗岩。本文所研究的火山岩出露于奥陶系南碧沟组中。野外剖面(自东向西)可依次观察到砾岩、流纹岩(图 2a)、石英砂岩、黑云

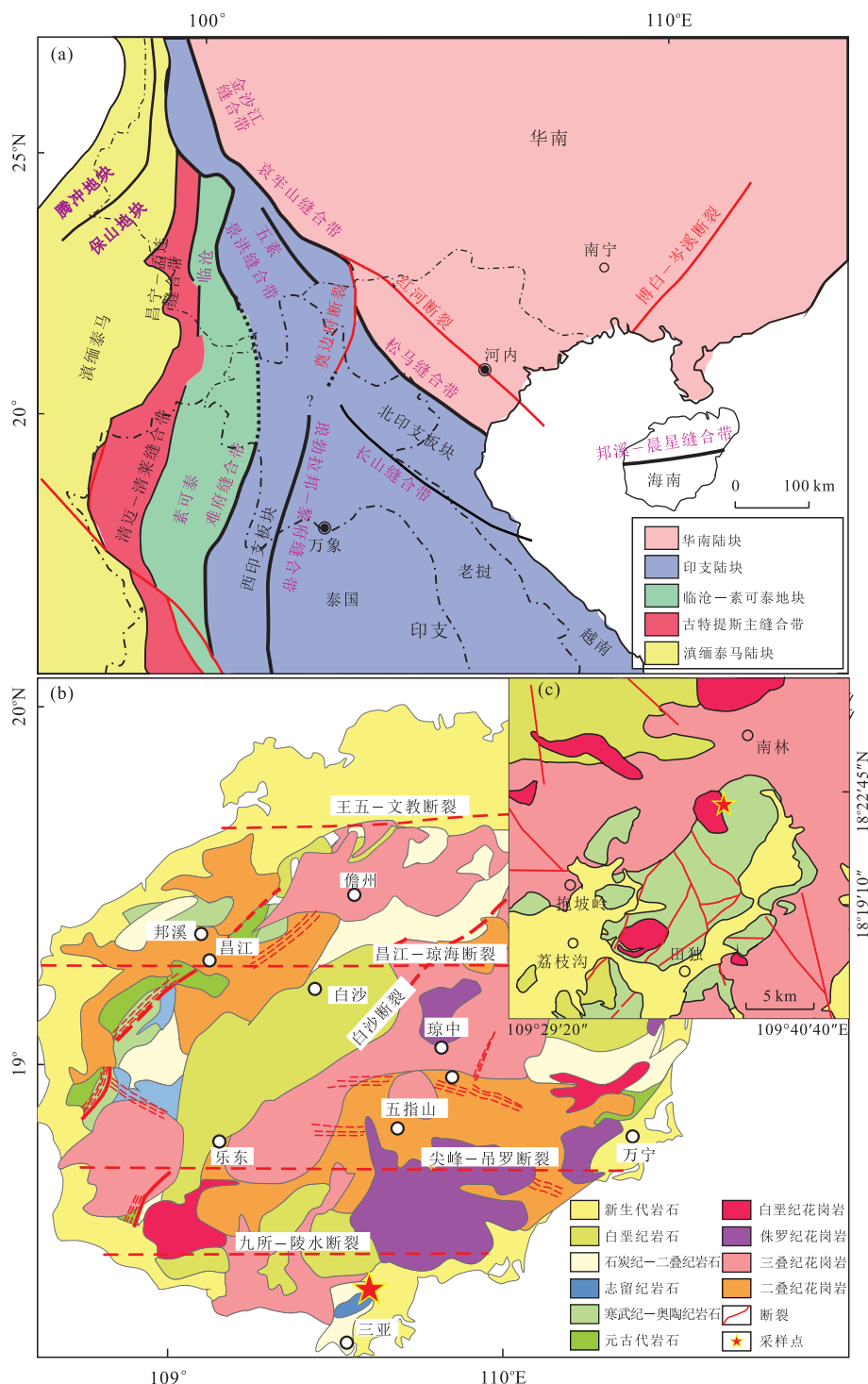


图1 东南亚地区构造划分(a)、海南岛地质简图(b)和研究区地质概况及采样点位置(c)

Fig.1 Tectonic outline of Southeast Asia (a), geological sketch of Hainan Island (b) and geological sketch of the study area showing the sampling location (c)

图a据Wang et al.(2010, 2018)修改;图b据Zhang et al.(2011)修改

母花岗岩、火山集块岩(图2e)、凝灰岩(图2c)以及层间砾岩,其中的酸性火山岩被上覆的砾岩角度不整合覆盖。野外观察流纹岩为浅红褐色,颗粒较细,易破碎;凝灰岩为浅紫灰色,风化较强;火山集块岩

为深灰黑色,出露体积较大。镜下观察表明流纹岩中的矿物斑晶主要为石英和长石,含少量黑云母;凝灰岩中可见石英和长石碎屑;火山集块岩的斑晶主要为石英和长石,基质为玻璃质。长石斑晶可见不同程

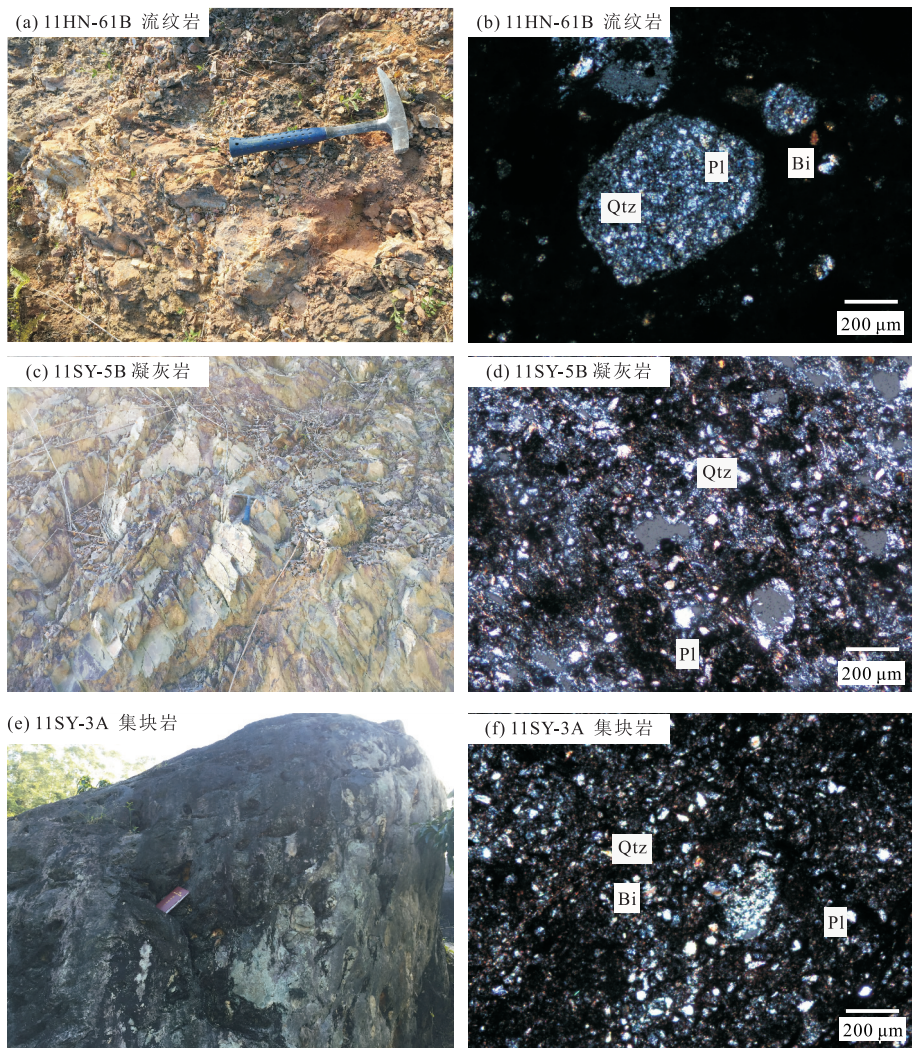


图 2 海南荔枝沟酸性火山岩野外照片(a,c,e)和岩石显微照片(b,d,f)

Fig.2 Field photographs (a,c,e) and photomicrographs (b,d,f) for the Liziogou felsic volcanic rocks in Hainan
Qtz.石英; Pl.斜长石; Bi.黑云母

度的绢云母化。

2 样品分析方法

通过人工重砂法和电磁选,从新鲜的样品中分选出无磁性重矿物样品。在双目镜下挑选出表面平整光洁、无裂隙、无包体、透明干净、形态较好的锆石颗粒,将其粘在双面胶上,并用混合固化剂的环氧树脂胶结,固化后细磨抛光制成样品靶。通过阴极发光(CL)探查锆石样品的内部结构,确定锆石的成因类型。锆石阴极发光图像由中山大学的 Carl ZEISS Σ IGMA 场发射扫描电镜完成。

锆石 U-Pb 同位素分析由中国科学院广州地球化学研究所同位素地球化学国家重点实验室的 ICP-MS Elan6100DRC 激光离子探针完成。详细的

分析步骤和数据处理方法参照 Xia *et al.*(2004), 数据处理软件使用 GLITTER4.4, 年龄计算及绘制相应图件使用 Ludwig(2003) 的 Isoplot 宏插件。

将岩石样品在无污染环境下粉碎至 200 目, 用于主微量元素和 Sr、Nd 同位素分析。全岩粉末样的主微量元素和 Sr-Nd 同位素组成分析在中国科学院广州地球化学研究所同位素地球化学国家重点实验室完成。主量元素分析采用 Rigaku RIX 2000 型荧光光谱仪(XRF)分析, 分析精度优于 1%~5%, 详细分析方法见 Li *et al.*(2005)。微量元素分析采用 PE Elan 6000 型电感耦合等离子体质谱仪(ICP-MS), 仪器分析精度优于 2%~5%, 具体分析流程和方法见刘颖等(1996)。Sr 和 Nd 同位素组成分析采用 Neptune 多接收等离子质谱仪(MC-ICP-MS)进行⁸⁷Sr/⁸⁶Sr 和¹⁴³Nd/¹⁴⁴Nd 比值测试。测定过程中

表1 海南荔枝沟酸性火山岩样品(11SY-3A) LA-ICP-MS 锆石 U-Pb 定年结果

Table 1 LA-ICP-MS U-Pb zircon geochronological data for the Lizhigou felsic volcanic rocks in Hainan

| 样品编号 | Th | U | Th/U | $^{207}\text{Pb}/^{206}\text{Pb}$ | 1σ | $^{207}\text{Pb}/^{235}\text{U}$ | 1σ | |
|------------|----------------------------------|-----------|-----------------------------------|-----------------------------------|----------------------------------|----------------------------------|----------------------------------|-----------|
| 11SY-3A-01 | 574 | 898 | 0.64 | 0.053 76 | 0.001 63 | 0.286 10 | 0.008 73 | |
| 11SY-3A-02 | 450 | 1 023 | 0.44 | 0.056 24 | 0.001 70 | 0.298 14 | 0.009 07 | |
| 11SY-3A-03 | 192 | 872 | 0.22 | 0.058 33 | 0.002 03 | 0.301 60 | 0.010 89 | |
| 11SY-3A-04 | 386 | 942 | 0.41 | 0.061 80 | 0.001 87 | 0.328 12 | 0.010 00 | |
| 11SY-3A-05 | 432 | 733 | 0.59 | 0.055 28 | 0.001 67 | 0.276 96 | 0.008 39 | |
| 11SY-3A-06 | 521 | 803 | 0.65 | 0.052 33 | 0.001 57 | 0.285 16 | 0.008 71 | |
| 样品编号 | $^{206}\text{Pb}/^{238}\text{U}$ | 1σ | $^{207}\text{Pb}/^{206}\text{Pb}$ | 1σ | $^{207}\text{Pb}/^{235}\text{U}$ | 1σ | $^{206}\text{Pb}/^{238}\text{U}$ | 1σ |
| 11SY-3A-01 | 0.038 62 | 0.001 18 | 361 | 64 | 255 | 7 | 244 | 7 |
| 11SY-3A-02 | 0.038 45 | 0.001 16 | 461 | 67 | 265 | 7 | 243 | 7 |
| 11SY-3A-03 | 0.037 43 | 0.001 17 | 543 | 76 | 268 | 8 | 237 | 7 |
| 11SY-3A-04 | 0.038 56 | 0.001 18 | 733 | 60 | 288 | 8 | 244 | 7 |
| 11SY-3A-05 | 0.036 37 | 0.001 11 | 433 | 73 | 248 | 7 | 230 | 7 |
| 11SY-3A-06 | 0.039 53 | 0.001 21 | 298 | 70 | 255 | 7 | 250 | 7 |

的质量分馏效应分别采用 $^{87}\text{Sr}/^{86}\text{Sr} = 0.119\ 4$ 和 $^{143}\text{Nd}/^{144}\text{Nd} = 0.721\ 9$ 进行校正.详细分析测试流程见 Yang *et al.* (2006).

3 LA-ICP-MS 锆石 U-Pb 年代学测试结果

分析的锆石样品 11SY-3A 为海南荔枝沟流纹岩,相关的同位素比值结果和年龄结果列于表 1 中.锆石 U 和 Th 的含量分别为 $733 \times 10^{-6} \sim 1 023 \times 10^{-6}$ 和 $192 \times 10^{-6} \sim 574 \times 10^{-6}$;锆石 Th/U 比值为 $0.22 \sim 0.65$,大部分大于 0.4,其 CL 图像显示锆石形态完整,有明显的振荡韵律环带结构(图 3a),为典型的岩浆成因锆石.其中 6 个锆石测点的 $^{206}\text{Pb}/^{238}\text{U}$

谐和年龄在 $230 \sim 250\text{ Ma}$ 之间,均靠近谐和曲线(图 3b).其加权平均年龄为 $241 \pm 6\text{ Ma}$, MSWD = 0.9,时代为中三叠世,代表了该套酸性火山岩的形成时间.

4 主微量元素及 Sr-Nd 同位素特征

荔枝沟地区酸性火山岩的主、微量元素和同位素分析结果列于表 2 中.11 个荔枝沟地区酸性火山岩样品烧失量为 $0.55\% \sim 2.25\%$, SiO_2 含量为 $72.34\% \sim 77.83\%$,具有低含量的 TiO_2 ($0.34\% \sim 0.54\%$), MgO ($0.54\% \sim 1.27\%$) 以及较高含量的 Al_2O_3 ($10.51\% \sim 13.53\%$), K_2O ($2.85\% \sim 4.85\%$) 和 Na_2O ($1.75\% \sim 3.79\%$) 的含量较高,全碱含量 ($\text{K}_2\text{O} + \text{Na}_2\text{O}$) 为 $5.83\% \sim 8.26\%$, $\text{Mg}^\#$ 值为 $11 \sim$

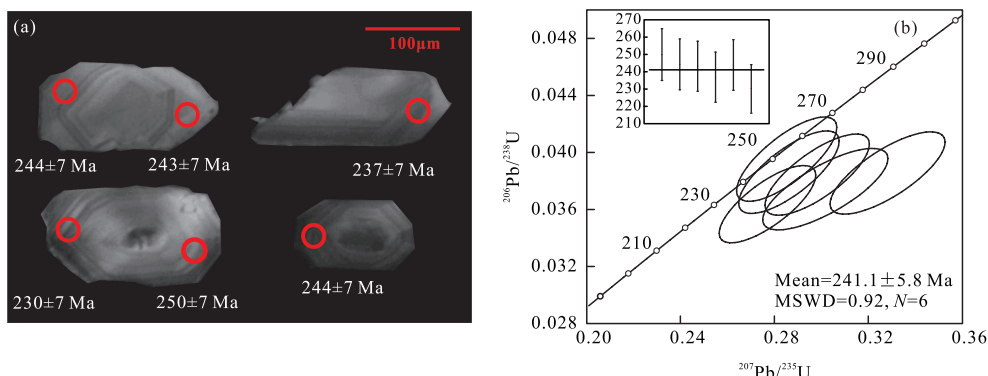
图3 荔枝沟酸性火山岩(11SY-3A)锆石 CL、测试点位及 $^{206}\text{Pb}/^{238}\text{U}$ 表观年龄(a)和锆石 U-Pb 谐和图(b)

Fig.3 CL images, dating spots and $^{206}\text{Pb}/^{238}\text{U}$ apparent age (a) of the zircons and U-Pb concordia diagram for the Lizhigou felsic volcanic rocks (11SY-3A) (b)

表 2 海南荔枝沟地区酸性火山岩主量元素(%)、微量元素(10^{-6})和 Sr-Nd 同位素组成分析结果Table 2 Major oxides (%), trace elements (10^{-6}) and Sr-Nd isotopic analytical results for the Lizhigou felsic volcanic rocks in Hainan

| 样品编号 | 11HN-61B | 11SY-3A | 11SY-3B | 11SY-3C | 11SY-3D | 11SY-3E | 11SY-3F | 11SY-3G | 11SY-5B | 11SY-5C |
|--|----------|-----------|---------|-----------|---------|---------|-----------|---------|---------|---------|
| SiO ₂ | 76.92 | 74.83 | 71.61 | 70.51 | 74.03 | 71.06 | 71.31 | 75.56 | 74.01 | 74.34 |
| TiO ₂ | 0.35 | 0.36 | 0.46 | 0.39 | 0.49 | 0.51 | 0.43 | 0.33 | 0.53 | 0.51 |
| Al ₂ O ₃ | 11.70 | 10.38 | 11.38 | 10.95 | 12.07 | 12.74 | 10.99 | 10.31 | 13.07 | 13.43 |
| Fe ₂ O ₃ | 2.20 | 2.97 | 3.20 | 3.48 | 2.60 | 3.17 | 2.83 | 2.65 | 3.47 | 3.50 |
| MgO | 1.73 | 3.08 | 3.54 | 3.68 | 2.61 | 3.35 | 3.40 | 2.74 | 2.32 | 2.37 |
| CaO | 0.62 | 2.66 | 3.19 | 4.16 | 1.13 | 1.70 | 3.69 | 2.54 | 0.29 | 0.32 |
| K ₂ O | 4.73 | 2.79 | 3.40 | 3.01 | 4.61 | 4.76 | 4.02 | 2.98 | 3.78 | 3.80 |
| Na ₂ O | 0.53 | 0.89 | 0.76 | 0.76 | 0.97 | 0.85 | 0.91 | 0.89 | 1.25 | 0.87 |
| MnO | 0.01 | 0.03 | 0.04 | 0.05 | 0.02 | 0.02 | 0.04 | 0.03 | 0.01 | 0.01 |
| P ₂ O ₅ | 0.04 | 0.04 | 0.06 | 0.06 | 0.06 | 0.06 | 0.08 | 0.05 | 0.10 | 0.09 |
| L.O.I | 0.98 | 1.31 | 1.68 | 2.25 | 0.79 | 1.10 | 1.65 | 1.30 | 0.60 | 0.55 |
| Total | 99.81 | 99.35 | 99.31 | 99.3 | 99.38 | 99.33 | 99.36 | 99.37 | 99.44 | 99.79 |
| Mg [#] | 32 | 32 | 37 | 32 | 30 | 42 | 35 | 39 | 33 | 11 |
| A/CNK | 1.65 | 1.22 | 1.12 | 1.01 | 1.45 | 1.30 | 0.99 | 1.25 | 2.05 | 2.07 |
| A/NK | 1.81 | 2.82 | 2.74 | 2.91 | 2.16 | 2.27 | 2.23 | 2.67 | 2.60 | 2.88 |
| Sc | 7.04 | 5.09 | 6.32 | 5.97 | 7.33 | 9.80 | 7.33 | 6.23 | | |
| V | 39.7 | 25.6 | 29.8 | 26.3 | 33.8 | 46.0 | 36.8 | 29.8 | | |
| Cr | 20.7 | 27.1 | 34.0 | 25.3 | 34.6 | 30.6 | 36.1 | 23.0 | | |
| Co | 3.99 | 6.33 | 5.69 | 5.41 | 5.20 | 7.23 | 6.38 | 6.00 | | |
| Ni | 5.78 | 12.80 | 13.50 | 11.20 | 12.30 | 16.50 | 19.60 | 23.00 | | |
| Rb | 124.0 | 84.6 | 113.0 | 93.8 | 115.0 | 139.0 | 105.0 | 97.0 | | |
| Sr | 82.9 | 76.6 | 95.9 | 84.9 | 62.0 | 67.3 | 89.3 | 76.9 | | |
| Y | 9.2 | 13.2 | 22.9 | 22.9 | 33.0 | 20.8 | 23.4 | 23.3 | | |
| Zr | 186 | 178 | 246 | 205 | 412 | 221 | 219 | 227 | | |
| Nb | 9.10 | 7.19 | 9.64 | 8.19 | 10.50 | 11.20 | 9.10 | 8.66 | | |
| Ba | 562 | 709 | 675 | 543 | 1 090 | 800 | 989 | 474 | | |
| La | 20.2 | 19.1 | 25.7 | 29.1 | 37.4 | 26.9 | 26.9 | 23.1 | | |
| Ce | 41.2 | 35.5 | 54.8 | 60.0 | 68.4 | 55.2 | 55.7 | 52.6 | | |
| Pr | 3.75 | 3.99 | 6.19 | 6.90 | 8.52 | 6.28 | 6.54 | 5.88 | | |
| Nd | 13.3 | 15.4 | 24.9 | 26.1 | 32.6 | 24.9 | 26.0 | 24.5 | | |
| Sm | 2.10 | 3.17 | 5.27 | 5.33 | 6.83 | 5.05 | 5.67 | 5.12 | | |
| Eu | 0.40 | 0.64 | 0.88 | 0.91 | 1.09 | 0.77 | 0.86 | 0.74 | | |
| Gd | 1.54 | 2.82 | 4.35 | 4.78 | 6.16 | 3.73 | 4.29 | 3.86 | | |
| Tb | 0.25 | 0.43 | 0.75 | 0.81 | 1.00 | 0.63 | 0.63 | 0.63 | | |
| Dy | 1.23 | 2.50 | 4.43 | 4.70 | 6.17 | 3.71 | 3.78 | 3.64 | | |
| Ho | 0.29 | 0.46 | 0.84 | 0.88 | 1.13 | 0.79 | 0.73 | 0.78 | | |
| Er | 1.01 | 1.60 | 2.56 | 2.66 | 3.59 | 2.43 | 2.31 | 2.39 | | |
| Tm | 0.17 | 0.26 | 0.40 | 0.39 | 0.53 | 0.36 | 0.32 | 0.36 | | |
| Yb | 1.37 | 1.76 | 2.50 | 2.61 | 3.50 | 2.44 | 2.25 | 2.35 | | |
| Lu | 0.26 | 0.30 | 0.41 | 0.42 | 0.55 | 0.39 | 0.37 | 0.36 | | |
| Hf | 4.58 | 5.38 | 6.68 | 6.05 | 11.60 | 6.14 | 5.76 | 5.72 | | |
| Ta | 0.50 | 0.82 | 0.71 | 0.66 | 0.83 | 0.78 | 0.62 | 0.56 | | |
| Pb | 10.7 | 15.2 | 15.8 | 11.3 | 16.2 | 16.2 | 19.1 | 15.1 | | |
| Th | 7.86 | 7.96 | 9.75 | 8.87 | 12.10 | 10.00 | 8.36 | 8.04 | | |
| U | 1.89 | 1.81 | 2.57 | 2.30 | 3.12 | 2.41 | 2.37 | 2.09 | | |
| Eu/Eu [*] | 0.65 | 1.38 | 1.72 | 2.04 | 1.98 | 1.54 | 1.59 | 1.74 | | |
| (La/Yb) _N | 26.6 | 18.8 | 35.1 | 39.5 | 39.3 | 31.9 | 41.9 | 43.8 | | |
| (Gd/Yb) _N | 0.58 | 0.56 | 1.18 | 1.33 | 1.36 | 1.01 | 1.18 | 1.39 | | |
| ⁸⁷ Rb/ ⁸⁶ Sr | | 3.209 | | 3.209 | | | 3.417 | | | |
| ¹⁴⁷ Sm/ ¹⁴⁴ Nd | | 0.124 | | 0.124 | | | 0.132 | | | |
| ⁸⁷ Sr/ ⁸⁶ Sr | | 0.751 057 | | 0.746 798 | | | 0.751 993 | | | |
| 2σ | | 6 | | 11 | | | 11 | | | |
| ¹⁴³ Nd/ ¹⁴⁴ Nd | | 0.511 947 | | 0.511 922 | | | 0.511 919 | | | |
| 2σ | | 6 | | 11 | | | 11 | | | |
| (⁸⁷ Sr/ ⁸⁶ Sr) _i | | 0.740 1 | | 0.735 8 | | | 0.740 3 | | | |
| ε _{Nd} (t) | | -11.3 | | -11.7 | | | -12.1 | | | |
| T _{DM2} (Ga) | | 1.67 | | 1.71 | | | 1.73 | | | |

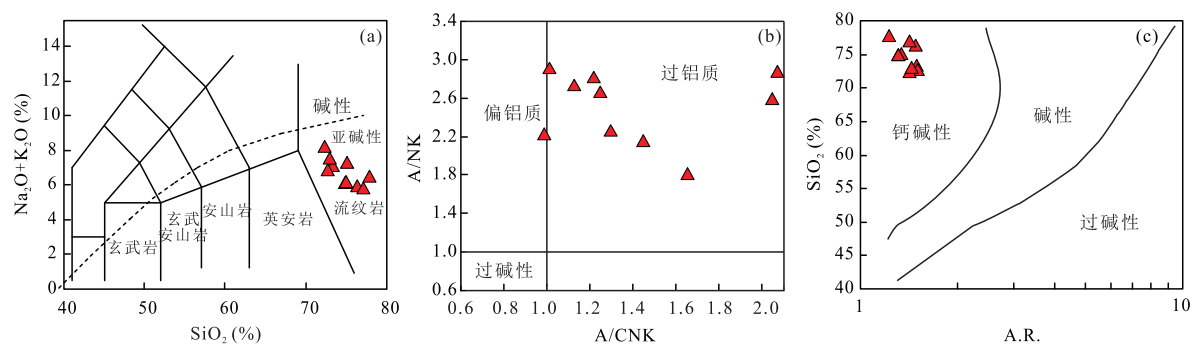
图4 荔枝沟酸性火山岩 TAS(a)、A/CNK—A/NK(b) 和 A.R.—SiO₂ 图解(c)

Fig.4 SiO₂ vs. Na₂O+K₂O(TAS) (a), A/NK vs. A/CNK (b) and A.R. vs. SiO₂ (c) classification diagrams for the Lihigou felsic volcanic rocks

图a据Maitre et al.(1989);图c据Wright(1969)

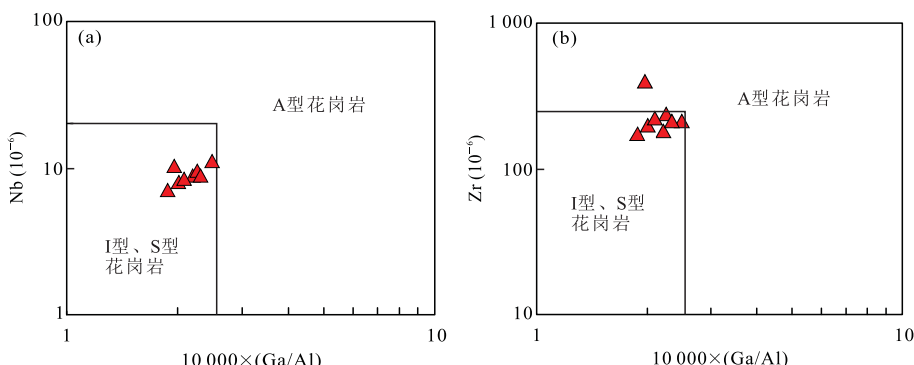


图5 荔枝沟酸性火山岩 10 000×Ga/Al—Nb (a) 和 10 000×(Ga/Al)—Zr 图解(b)

Fig.5 10 000×Ga/Al vs. Nb (a) and 10 000×Ga/Al vs. Zr (b) diagrams for the Lihigou felsic volcanic rocks

据Whalen et al.(1987)

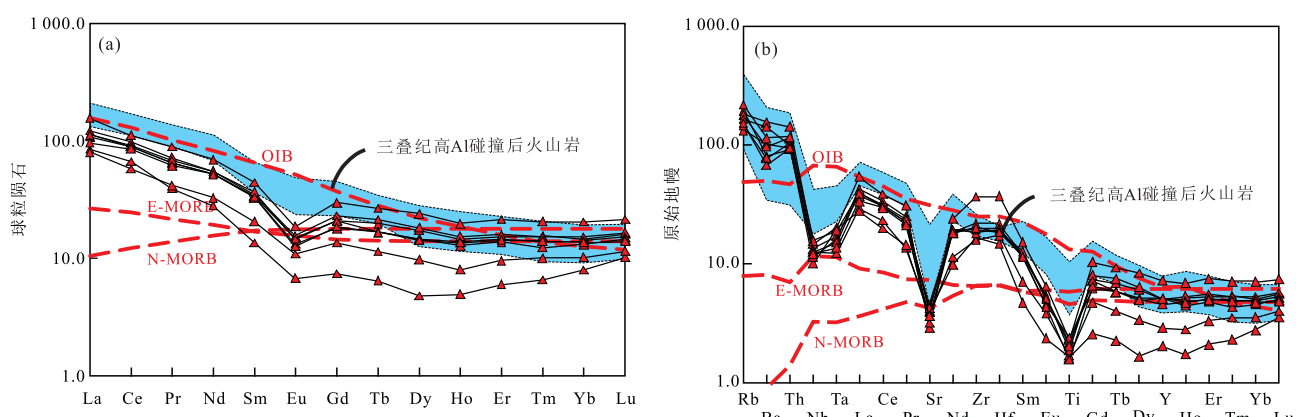


图6 荔枝沟酸性火山岩球粒陨石标准化稀土元素配分图(a)和标准化微量元素蛛网图(b)

Fig.6 Chondrite-normalized REE pattern(a) and primitive mantle-normalized spidergram (b) for the Lihigou felsic volcanic rocks
球粒陨石及原始地幔数据来自Sun and McDonough(1989),三叠纪高AI碰撞后火山岩数据来自Wang et al.(2010)

42. 在TAS图解中(图4a),样品皆落于亚碱性流纹岩区域内。样品的铝饱和指数(A/CNK)变化较大为0.99~2.07,大部分样品A/CNK>1.1(图4b)。在A.R.—SiO₂图解中(图4c),样品点都位于钙碱性区

域范围内,因此该套酸性岩浆岩属于钙碱性过铝质酸性火山岩。另外,样品的10 000×(Ga/Al)比值在1.87~2.48的范围内,且大部分样品点落于I或S型花岗岩的区域内(图5; Whalen et al., 1987),这

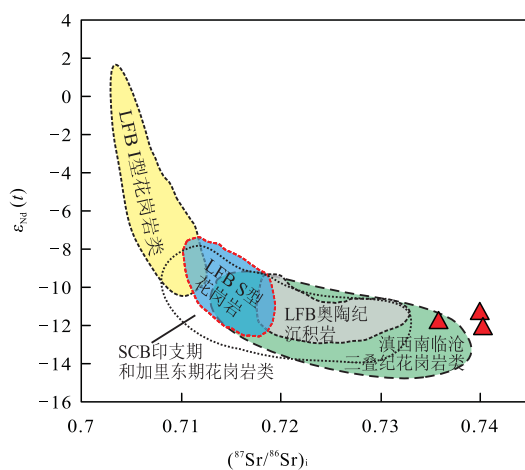
图 7 荔枝沟酸性火山岩 $(^{87}\text{Sr}/^{86}\text{Sr})_i-\epsilon_{\text{Nd}}(t)$ 图解

Fig.7 $(^{87}\text{Sr}/^{86}\text{Sr})_i$ vs. $\epsilon_{\text{Nd}}(t)$ diagram for the Lizhigou felsic volcanic rocks

拉克兰褶皱带(LFB)数据、华南陆块(SCB)印支期、加里东期花岗岩以及滇西南临沧三叠纪花岗岩数据来自 Healy *et al.* (2004); Wang *et al.* (2007, 2013, 2015) 和 Peng *et al.* (2013)

些特征表明所研究样品的性质与 S 型花岗岩接近, 同时分异指数 DI ($DI = Q + Or + Ab + Ne + Lc + Kp$) 为 $85.5 \sim 92.4$, 表明岩浆经历了高度分异。

荔枝沟酸性火山岩样品稀土元素 $\sum \text{REE}$ 变化于 $87 \times 10^{-6} \sim 177 \times 10^{-6}$. 在球粒陨石标准化图解(图 6a)上, 稀土元素配分曲线显示出 LREE 富集的右倾型配分模式, 样品轻、重稀土分异明显, $(\text{La/Yb})_N = 7.05 \sim 10.58$, $(\text{Gd/Yb})_N = 0.93 \sim 1.58$, Eu 负异常明显($\text{Eu/Eu}^* = 0.49 \sim 0.65$), 其配分特征类似澜沧江晚三叠世高 Al 碰撞后火山岩(Wang *et al.*, 2010). 在微量元素蛛网图上(图 6b), 荔枝沟酸性火山岩样品富集大离子亲石元素(如 Rb、Ba 等), 亏损高场强元素, 具有 Nb、Ta 和 Ti 的负异常, 其配分模式类似于岛弧火山岩. 3 个代表性样品均

具较低的全岩 Nd 同位素比值($^{143}\text{Nd}/^{144}\text{Nd} = 0.511\,919 \sim 0.511\,947$). 根据流纹岩形成年龄(241.1 Ma)计算得到的 $(^{87}\text{Sr}/^{86}\text{Sr})_i$ 初始值为 $0.735\,8 \sim 0.740\,3$, $\epsilon_{\text{Nd}}(t)$ 值为 $-11.3 \sim -12.1$, Nd 的二阶模式年龄 T_{DM2} 为 $1.67 \sim 1.73\text{ Ga}$. 在图 $(^{87}\text{Sr}/^{86}\text{Sr})_i-\epsilon_{\text{Nd}}(t)$ 中(图 7), 这些样品均靠近滇西地区临沧三叠纪花岗岩区(Peng *et al.*, 2013), 同时样品的 $\epsilon_{\text{Nd}}(t)$ 值与金沙江—哀牢山构造带内的晚三叠世酸性岩浆岩类似($\epsilon_{\text{Nd}}(t) = -11.4 \sim -10.6$, Liu *et al.*, 2015; $\epsilon_{\text{Nd}}(t) = -10.66 \sim -9.61$, Wang *et al.*, 2014).

5 讨论

5.1 酸性火山岩岩石成因

所研究的海南三亚荔枝沟地区酸性火山岩烧失量(LOI) 小于 3% ($0.55\% \sim 2.25\%$), 表明岩浆喷出后未经受强烈的风化和剥蚀. 在稀土元素配分图和微量元素蛛网图中, 样品具有明显的 Ba、Sr、Ti 和 Eu 负异常特征, 说明岩浆在演化过程中可能存在碱性长石、斜长石和黑云母的分离结晶作用. 另外, 样品点在 La-La/Sm 图解(图 8a)中的趋势显示该套酸性火山岩具有分离结晶作用, 在 Sr-Rb 图解(图 8b)和 Sr-Ba 图解(图 8c)中均显示出一定程度的黑云母和斜长石分离结晶的趋势.

如前所述, 大部分样品的 A/CNK 值较高($A/\text{CNK} > 1.1$), 为过铝质岩石. 现有资料表明, 富硅的过铝质岩浆岩的形成原因有:(1)富铝变质岩(如片岩和片麻岩)的部分熔融(Wang *et al.*, 2007);(2)角闪岩在富水条件下部分熔融(Ellis and Thompson, 1986);(3)贫铝质岩浆的分异(Zen, 1986). 然而, 由(2)和(3)形成的岩浆岩具有偏铝质、富集 Na

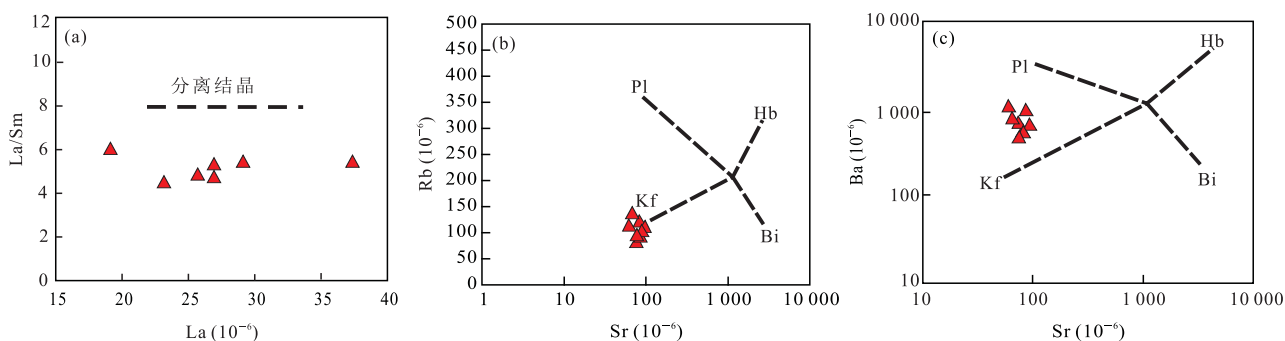


图 8 荔枝沟酸性火山岩 La-La/Sm (a)、Sr-Rb (b) 和 Sr-Ba 图解(c)

Fig.8 La vs. La/Sm (a), Sr vs. Rb (b) and Sr vs. Ba (c) diagrams for the Lizhigou felsic volcanic rocks

和 Sr 的特征 (Zen, 1986), 这与所研究的荔枝沟酸性火山岩的过铝质和亏损 Sr 的特征不相符。一般情况下, 高级变质岩在富水条件下的深熔作用能产生 2%~5% 的熔体 (Zen, 1986; Patino Douce *et al.*, 1990), 而这种情况形成的岩浆岩出露范围较小。所研究的样品具有与临沧三叠纪花岗岩相似的地球化学特征, 在 $(^{87}\text{Sr}/^{86}\text{Sr})_i - \epsilon_{\text{Nd}}(t)$ 图中接近滇西南临沧三叠纪 S 型花岗岩区域 (图 7)。已有研究认为, 临沧三叠纪花岗岩源自中上地壳变沉积岩的部分熔融 (Peng *et al.*, 2013), 因此, 推测荔枝沟酸性火山岩可能源于富铝变质岩的部分熔融。

酸性火山岩的成分与其源区密切相关。由于熔体中 $\text{CaO}/\text{Na}_2\text{O}$ 比值的大小主要依赖于斜长石/粘土的比值, 而与温度和压力无关, 因此 $\text{CaO}/\text{Na}_2\text{O}$ 比值能够较好地指示源区的成分 (Sylvester, 1998)。所研究样品的 $\text{CaO}/\text{Na}_2\text{O}$ 比值均大于 0.3, 符合富斜长石贫粘土源区产生的强过铝质花岗岩的 $\text{CaO}/\text{Na}_2\text{O}$ 比值范围 (>0.3), 非贫斜长石富粘土源区产生的强过铝质花岗岩 ($\text{CaO}/\text{Na}_2\text{O}$ 比值 <0.3 ; Patino Douce and Johnsto, 1991)。同时, 在 $\text{Rb}/\text{Sr}-\text{Rb}/\text{Ba}$ 图解中 (图 9a), 样品全部落于贫粘土源岩的区域; 在 $(\text{Al}_2\text{O}_3 + \text{FeO}^T + \text{MgO} + \text{TiO}_2) - \text{Al}_2\text{O}_3/(\text{FeO}^T + \text{MgO} + \text{TiO}_2)$ 图解中 (图 9b), 部分样品点落于杂砂岩和角闪岩部分熔融的重叠区, 但大多数样品落入杂砂岩部分熔融的区域。该特征结合部分样品具有较高的 $\text{Mg}^{\#}(>30)$ 值, 可以推测荔枝沟酸性火山岩的源区主要为富斜长石贫粘土杂砂岩源区, 同时可能有一定量变火成岩的参与。

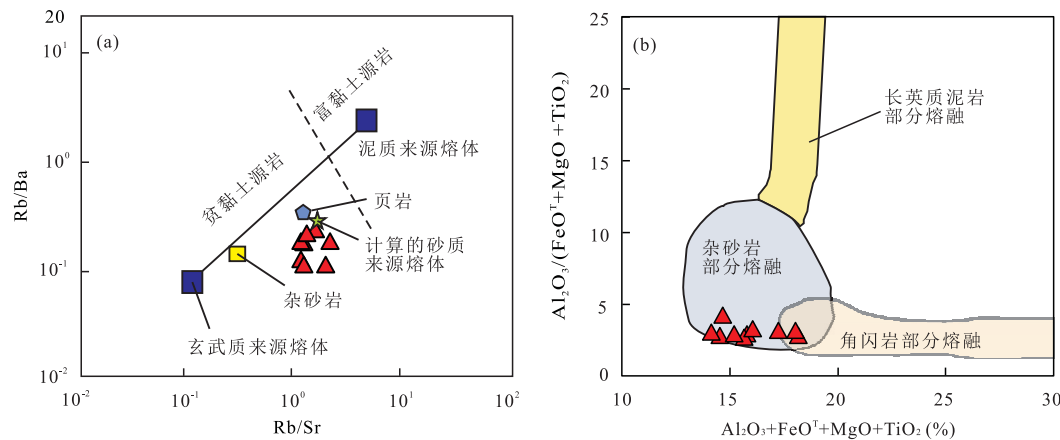


图 9 荔枝沟酸性火山岩 $\text{Rb}/\text{Sr}-\text{Rb}/\text{Ba}$ (a) 和 $(\text{Al}_2\text{O}_3 + \text{FeO}^T + \text{MgO} + \text{TiO}_2) - \text{Al}_2\text{O}_3/(\text{FeO}^T + \text{MgO} + \text{TiO}_2)$ 图解 (b)

Fig.9 Rb/Sr vs. Rb/Ba (a) and $(\text{Al}_2\text{O}_3 + \text{FeO}^T + \text{MgO} + \text{TiO}_2) - \text{Al}_2\text{O}_3/(\text{FeO}^T + \text{MgO} + \text{TiO}_2)$ (b) diagrams for the Lizhigou felsic volcanic rocks

图 a 据 Sylvester (1998); 图 b 据 Wang *et al.* (2016)

温度升高能够使含钛矿物 (如钛铁矿和黑云母) 更易分解, 导致更多的 TiO_2 进入岩浆, 因此 $\text{Al}_2\text{O}_3/\text{TiO}_2$ 比值能够很好地指示强过铝质花岗岩岩浆形成的温度 (Sylvester, 1998)。当 $\text{Al}_2\text{O}_3/\text{TiO}_2$ 比值较高时 (大于 100) 形成温度为低温 ($825\sim900\text{ }^\circ\text{C}$), 当 $\text{Al}_2\text{O}_3/\text{TiO}_2$ 比值较低时 (小于 100) 形成温度为高温 ($900\sim950\text{ }^\circ\text{C}$) (Sylvester, 1998)。荔枝沟酸性火山岩样品的 $\text{Al}_2\text{O}_3/\text{TiO}_2$ 比值均小于 100, 反映其部分熔融的温度为高温 ($>875\text{ }^\circ\text{C}$), 属高温型强过铝质酸性火山岩。高压型和高温型强过铝质花岗岩的主要区别在于前者形成的温度较低 ($<875\text{ }^\circ\text{C}$), 其诱发地壳物质熔融的热动力因素是地壳增厚, 而后者的形成温度较高 ($>875\text{ }^\circ\text{C}$), 是通过玄武质岩浆的底侵作用导致地壳物质重熔形成的 (钟长汀等, 2007)。综上所述, 荔枝沟酸性火山岩是中上地壳的变沉积岩受到玄武质岩浆底侵作用而发生部分熔融、后经历一定程度的分离结晶作用的产物。

5.2 构造意义

荔枝沟酸性岩浆岩为钙碱性岩, 具有富集大离子亲石元素、亏损高场强元素的特征。在构造环境判别图中 (图 10), 本次研究的样品点落于碰撞后火山岩的区域范围, 显示荔枝沟酸性火山岩形成于碰撞后的构造环境。除本文报道的海南三亚地区 241 Ma 酸性岩浆岩之外, 海南岛还分布有同一时期的中基性岩浆岩, 比如: 在三亚地区的石榴霓辉石正长岩 (244 Ma; 谢才富等, 2005); 万宁地区的辉长岩和辉绿岩脉 (240 Ma; 唐立梅, 2010); 分界洲地区的 A 型正长岩类 (231 Ma; 唐立梅, 2010); 陵水—龙滚断

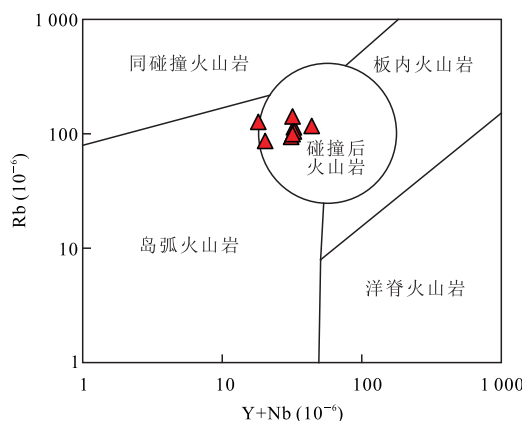


图 10 荔枝沟酸性火山岩 $Y+Nb$ -Rb 构造判别图解
Fig.10 $Y+Nb$ vs. Rb discrimination diagram for the
Lizhigou felsic volcanic rocks
据 Pearce (1996)

裂两侧及白沙断裂东南侧中三叠世的正长岩和花岗岩组合(周佐民等, 2011). 这些关于碱性岩、辉长岩和辉绿岩的研究表明海南岛在 240 Ma 左右已进入后造山伸展阶段. 根据野外观察发现, 荔枝沟酸性火山岩被上覆的上三叠统砾岩角度不整合覆盖, 暗示了华南陆块和印支陆块之间的碰撞在晚三叠世之前已经结束(Jian et al., 2009; Fan et al., 2010; Liu et al., 2014).

越来越多的研究表明, 在晚古生代至早中生代时期, 海南岛的构造演化与古特提斯洋的闭合及印支、华南陆块的拼合有着密切的联系. Li et al. (2002) 和 He et al. (2017) 对邦溪—晨星地区石炭纪变基性岩与金沙江—哀牢山—松马缝合带内的岩浆记录进行对比, 认为沿金沙江—哀牢山—松马带和邦溪—晨溪带发育了弧后盆地. Li et al. (2006) 和陈新跃等(2011)在五指山地区获得了 267~262 Ma 与俯冲相关的 I 型花岗片麻岩. 唐立梅等(2013)认为 238~234 Ma 的兴隆双峰式侵入岩的成因与古特提斯洋的俯冲闭合有关. 相应地沿金沙江—哀牢山—松马构造带分布有大量的晚二叠世至三叠纪的岩浆岩. Zi et al. (2012) 在白马雪山识别出了 250 Ma 的闪长岩和英云闪长岩组合. Liu et al. (2015) 在哀牢山构造带发现了 247 Ma 的狗头坡和通天阁淡色花岗岩, 其中通天阁花岗岩的 $\epsilon_{Nd}(t)$ 值为 -11.4~-10.6, 与所研究的荔枝沟酸性火山岩的 $\epsilon_{Nd}(t)$ 值接近. Liu et al. (2017) 还在下关地区识别出了形成于 233~229 Ma 碰撞后的强过铝质 S 型花岗质岩, 该套花岗质岩具有富集的 Sr-Nd 同位素组成, $\epsilon_{Nd}(t)$ 小于 -10. 最近 Wang et al. (2018) 研究表明,

金沙江—哀牢山—松马分支洋/弧后盆地的同碰撞和后碰撞时间分别为 247 Ma 和 237 Ma. 以上认识表明在中—晚三叠世时期, 金沙江—哀牢山—松马构造带已处于同碰撞—后碰撞的构造背景. 因此海南岛在二叠纪末—中三叠世的构造演化过程可与古特提斯构造域在滇西的演化进行对比. 除了岩浆记录外, 研究者们也对海南岛和印支陆块东北部地区的韧性剪切带进行了对比研究, 并在琼中和琼西公爱地区发现了 NW 向右旋走滑韧性剪切带, 其糜棱岩同构造期云母的 ^{40}Ar - ^{39}Ar 坪年龄为 242~245 Ma, 而在印支陆块北部松马、岘港—溪山和 Song Ca-Rao Nay 等地发现的韧性剪切带, 其构造特征和变形年龄(254~240 Ma)与前者一致(Lepvrier et al., 2004; 陈新跃等, 2006; Zhang et al., 2011). 野外观察表明荔枝沟酸性火山岩被上覆的上三叠统砾岩角度不整合所覆盖, 而研究者们在金沙江—哀牢山地区发现中至上三叠统的火山岩序列也被上三叠统一碗水组砾岩不整合覆盖(Peng et al., 2006; Zi et al., 2012; Wang et al., 2018). 荔枝沟地区酸性火山岩的地化特征也表明其源区为变沉积物, 具有碰撞后岩浆作用的主要特征, 其形成年龄(241.1 Ma)符合三江地区一般认为的碰撞后的岩浆作用时间, 与金沙江—哀牢山—松马构造带内碰撞后岩浆作用在时空上相吻合(Liu et al., 2014). 结合海南岛二叠纪俯冲相关的 I 型花岗岩, 现有的资料暗示了华南和印支陆块之间的俯冲于早二叠世已开始, 并在 240 Ma 左右进入到后碰撞环境. 此时期华南陆块和印支陆块碰撞后发生板片拆沉、软流圈上涌, 导致上地壳物质发生部分熔融, 从而形成了荔枝沟酸性火山岩(Liu et al., 2014, 2017; Wang et al., 2018).

6 结论

(1) 海南岛荔枝沟地区酸性火山岩 LA-ICP-MS 锆石 U-Pb 年龄为 241.1 ± 5.8 Ma, 为中三叠世;

(2) 荔枝沟地区酸性火山岩具有高 Al_2O_3 和全碱含量、富集轻稀土元素和大离子亲石元素、亏损 Nb、Ta 和 Ti 等高场强元素等特征, 为变沉积岩部分熔融并经历一定程度的分离结晶的产物;

(3) 荔枝沟酸性火山岩形成于碰撞闭合后的伸展环境, 与碰撞后板片拆沉、软流圈上涌有关, 并可以与金沙江—哀牢山—松马带相关的中—晚三叠世岩浆岩进行对比.

致谢: 野外样品采集以及室内岩石分析工作得到

了毕明威博士后和张立敏博士的帮助,在此致以最诚挚的谢意。感谢审稿专家给出了宝贵的审稿意见。

References

- Bureau of Geology and Mineral Resources of Guangdong Province, 1988. Regional Geology of Guangdong Province. Geological Publishing House, Beijing (in Chinese).
- Chen, X. Y., Wang, Y. J., Fan, W. M., et al., 2011. Zircon LA-ICP-MS U-Pb Dating of Granitic Gneisses from Wuzhishan Area, Hainan, and Geological Significances. *Geochimica*, 40 (5): 454–463 (in Chinese with English abstract).
- Chen, X. Y., Wang, Y. J., Han, H. P., et al., 2014. Geochemical and Geochronological Characteristics of Triassic Basic Dikes in SW Hainan Island and Its Tectonic Implications. *Journal of Jilin University (Earth Science Edition)*, 44(3): 835–847 (in Chinese with English abstract).
- Chen, X. Y., Wang, Y. J., Wei, M., et al., 2006. Microstructural Characteristics of the NW-Trending Shear Zones of Gong'ai Region in Hainan Island and Its ^{40}Ar - ^{39}Ar Geochronological Constraints. *Geotectonica et Metallogenesis*, 30(3): 312–319 (in Chinese with English abstract).
- Ellis, D. J., Thompson, A. B., 1986. Subsolidus and Partial Melting Reactions in the Quartz-Excess $\text{CaO} + \text{MgO} + \text{Al}_2\text{O}_3 + \text{SiO}_2 + \text{H}_2\text{O}$ System under Water-Excess and Water-Deficient Conditions to 10 kb: Some Implications for the Origin of Peraluminous Melts from Mafic Rocks. *Journal of Petrology*, 27(1): 91–121.
- Fan, W. M., Wang, Y. J., Zhang, A. M., et al., 2010. Permian Arc-back-Arc Basin Development along the Ailaoshan Tectonic Zone: Geochemical, Isotopic and Geochronological Evidence from the Mojiang Volcanic Rocks, Southwest China. *Lithos*, 119(3–4): 553–568. <https://doi.org/10.1016/j.lithos.2010.08.010>
- He, H. Y., Wang, Y. J., Qian, X., et al., 2018. The Bangxi-Chenxing Tectonic Zone in Hainan Island (South China) as the Eastern Extension of the Song Ma-Ailaoshan Zone: Evidence of Late Paleozoic and Triassic Igneous Rocks. *Journal of Asian Earth Sciences*, 164: 274–291.
- He, H. Y., Wang, Y. J., Zhang, Y. H., et al., 2017. Fingerprints of the Paleotethyan Back-Arc Basin in Central Hainan, South China: Geochronological and Geochemical Constraints on the Carboniferous Metabasites. *International Journal of Earth Sciences*, 107(2): 553–570.
- Healy, B., Collins, W. J., Richards, S. W., 2004. A Hybrid Origin for Lachlan S-Type Granites: The Murrumbidgee Batholith Example. *Lithos*, 78 (1–2): 197–216. <https://doi.org/10.1016/j.lithos.2004.04.047>
- Hu, N., Zhang, R. J., Feng, S. N., 2002. Study on Devonian-Carboniferous Boundary in Hainan Island, South China. *Chinese Journal of Geology*, 37(3): 313–319, 387 (in Chinese with English abstract).
- Jian, P., Liu, D. Y., Kröner, A., et al., 2009. Devonian to Permian Plate Tectonic Cycle of the Paleo-Tethys Orogen in Southwest China (II): Insights from Zircon Ages of Ophiolites, Arc/back-Arc Assemblages and within-Plate Igneous Rocks and Generation of the Emeishan CFB Province. *Lithos*, 113 (3–4): 767–784. <https://doi.org/10.1016/j.lithos.2009.04.006>
- Lepvrier, C., Maluski, H., van Tich, V., et al., 2004. The Early Triassic Indosinian Orogeny in Vietnam (Truong Son Belt and Kontum Massif): Implications for the Geodynamic Evolution of Indochina. *Tectonophysics*, 393 (1–4): 87–118. <https://doi.org/10.1016/j.tecto.2004.07.030>
- Li, S. B., He, H. Y., Qian, X., et al., 2018. Carboniferous Arc Setting in Central Hainan: Geochronological and Geochemical Evidences on the Andesitic and Dacitic Rocks. *Journal of Earth Science*, 29 (2): 265–279. <https://doi.org/10.1007/s12583-017-0936-0>
- Li, S. X., Yun, Y., Fan, Y., et al., 2005. Zircon U-Pb Age and Its Geological Significance for Qiongzhong Pluton in Qiongzhong Area, Hainan Island. *Geotectonica et Metallogenesis*, 29(2): 227–233, 241 (in Chinese with English abstract).
- Li, X. H., Li, Z. X., Li, W. X., et al., 2006. Initiation of the Indosinian Orogeny in South China: Evidence for a Permian Magmatic Arc on Hainan Island. *The Journal of Geology*, 114 (3): 341–353. <https://doi.org/10.1086/501222>
- Li, X. H., Qi, C. S., Liu, Y., et al., 2005. Petrogenesis of the Neoproterozoic Bimodal Volcanic Rocks along the Western Margin of the Yangtze Block: New Constraints from Hf Isotopes and Fe/Mn Ratios. *Chinese Science Bulletin*, 50(21): 2481–2486.
- Li, X. H., Zhou, H. W., Chung, S. L., et al., 2002. Geochemical and Sm-Nd Isotopic Characteristics of Metabasites from Central Hainan Island, South China and Their Tectonic Significance. *The Island Arc*, 11(3): 193–205. <https://doi.org/10.1046/j.1440-1738.2002.00365.x>
- Li, X. H., Zhou, H. W., Ding, S. J., et al., 2000. Mid Ocean Ridge Metabasic Volcanic Rocks of Hainan Island: Paleo-Tethyan Oceanic Crust Slices? *Chinese Science Bulletin*, 45(1): 84–89 (in Chinese).
- Liu, H. C., Wang, Y. J., Cawood, P. A., et al., 2015. Record of Tethyan Ocean Closure and Indosinian Collision along the Ailaoshan Suture Zone (SW China). *Gondwana Research*, 27(3): 1292–1306.

- Liu, H.C., Wang, Y.J., Fan, W.M., et al., 2014. Petrogenesis and Tectonic Implications of Late-Triassic High $\epsilon_{\text{Nd}}(t)$ - $\epsilon_{\text{Hf}}(t)$ Granites in the Ailaoshan Tectonic Zone (SW China). *Science China Earth Sciences*, 57(9): 2181–2194. <https://doi.org/10.1007/s11430-014-4854-z>
- Liu, H.C., Wang, Y.J., Guo, X.F., et al., 2017. Late Triassic Post-Collisional Slab Break-off along the Ailaoshan Suture: Insights from OIB-Like Amphibolites and Associated Felsic Rocks. *International Journal of Earth Sciences*, 106(4): 1359–1373.
- Liu, Y., Liu, H.C., Li, X.H., 1996. Simultaneous and Precise Determination of 40 Trace Elements in Rock Samples Using ICP-MS. *Geochimica*, 25(6): 552–558 (in Chinese with English abstract).
- Long, W.G., Fu, C.R., Zhu, Y.H., 2002. Disintegration of the Baoban Group in Huangzhuling Area of Eastern Hainan Island. *Journal of Stratigraphy*, 26(3): 212–215 (in Chinese with English abstract).
- Long, W.G., Tong, J.N., Zhu, Y.H., et al., 2007. Discovery of the Permian in the Danzhou-Tunchang Area of Hainan Island and Its Geological Significance. *Geology and Mineral Resources of South China*, 23(1): 38–45 (in Chinese with English abstract).
- Ludwig, K. R., 2003. ISOPLOT 3.00: A Geochronological Toolkit for Microsoft Excel. Berkeley Geochronology Center, California, Berkeley.
- Ma, D.Q., Huang, X.D., Xiao, Z.F., et al., 1998. Crystallized Basement in Hainan Island: Sequence and Epoch of the Baoban Group. China University of Geosciences Press, Wuhan, 1–52 (in Chinese).
- Maitre, R.W.L., Bateman, P., Dudek, A., et al., 1989. A Classification of Igneous Rocks and Glossary of Terms. Blackwell Science Publication, Oxford.
- Patino Douce, A. E., Humphreys, E. D., Dana Johnston, A., 1990. Anatexis and Metamorphism in Tectonically Thickened Continental Crust Exemplified by the Sevier Hinterland, Western North America. *Earth and Planetary Science Letters*, 97(3–4): 290–315. [https://doi.org/10.1016/0012-821x\(90\)90048-3](https://doi.org/10.1016/0012-821x(90)90048-3)
- Patino Douce, A. E., Johnston, A. D., 1991. Phase Equilibria and Melt Productivity in the Pelitic System: Implications for the Origin of Peraluminous Granitoids and Aluminous Granulites. *Contributions to Mineralogy and Petrology*, 107(2): 202–218. <https://doi.org/10.1007/bf00310707>
- Pearce, J. A., 1996. Sources and Settings of Granitic Rocks. *Episodes*, 19: 120–125.
- Peng, T.P., Wang, Y.J., Fan, W.M., et al., 2006. SHRIMP Zircon U-Pb Geochronology of Early Mesozoic Felsic Igneous Rocks from the Southern Lancangjiang and Its Tectonic Implications. *Science China Earth Sciences*, 49(10): 1032–1042. <https://doi.org/10.1007/s11430-006-1032-y>
- Peng, T.P., Wilde, S.A., Wang, Y.J., et al., 2013. Mid-Triassic Felsic Igneous Rocks from the Southern Lancangjiang Zone, SW China: Petrogenesis and Implications for the Evolution of Paleo-Tethys. *Lithos*, 168–169: 15–32. <https://doi.org/10.1016/j.lithos.2013.01.015>
- Shen, B. Y., Liu, B., Liu, H. L., et al., 2016. Xiaomei Ductile Shear Zone on Hainan Island in a Nanoscale Perspective. *Earth Science*, 41(9): 1489–1498 (in Chinese with English abstract).
- Sun, S. S., McDonough, W. F., 1989. Chemical and Isotopic Systematics of Oceanic Basalts: Implications for Mantle Composition and Processes. *Geological Society, London, Special Publications*, 42(1): 313–345. <https://doi.org/10.1144/gsl.sp.1989.042.01.19>
- Sylvester, P.J., 1998. Post-Collisional Strongly Peraluminous Granites. *Lithos*, 45(1–4): 29–44. [https://doi.org/10.1016/s0024-4937\(98\)00024-3](https://doi.org/10.1016/s0024-4937(98)00024-3)
- Tang, L. M., 2010. Magmatic Evidence of Two Tectonic Extension Events during the Mesozoic in Hainan Island & Geodynamic Implications (Dissertation). Zhejiang University, Hangzhou (in Chinese with English abstract).
- Tang, L. M., Chen, H. L., Dong, C. W., et al., 2013. Middle Triassic Post-Orogenic Extension on Hainan Island: Chronology and Geochemistry Constraints of Bimodal Intrusive Rocks. *Science China Earth Science*, 43(3): 433–445 (in Chinese).
- Wang, B. D., Wang, L. Q., Chen, J. L., et al., 2014. Triassic Three-Stage Collision in the Paleo-Tethys: Constraints from Magmatism in the Jiangda-Deqen-Weixi Continental Margin Arc, SW China. *Gondwana Research*, 26(2): 475–491. <https://doi.org/10.1016/j.gr.2013.07.023>
- Wang, Y.J., Fan, W.M., Sun, M., et al., 2007. Geochronological, Geochemical and Geothermal Constraints on Petrogenesis of the Indosian Peraluminous Granites in the South China Block: A Case Study in the Hunan Province. *Lithos*, 96(3–4): 475–502. <https://doi.org/10.1016/j.lithos.2006.11.010>
- Wang, Y.J., He, H.Y., Cawood, P.A., et al., 2016. Geochronological, Elemental and Sr-Nd-Hf-O Isotopic Constraints on the Petrogenesis of the Triassic Post-Collisional Granitic Rocks in NW Thailand and Its Paleotethyan Implications. *Lithos*, 266–267: 264–286.
- Wang, Y.J., Li, S.B., Ma, L. Y., et al., 2015. Geochronological

- and Geochemical Constraints on the Petrogenesis of Early Eocene Metagabbroic Rocks in Nabang (SW Yunnan) and Its Implications on the Neotethyan Slab Subduction. *Gondwana Research*, 27(4):1474—1486.
- Wang, Y.J., Qian, X., Cawood, P.A., et al., 2018. Closure of the East Paleotethyan Ocean and Amalgamation of the Eastern Cimmerian and Southeast Asia Continental Fragments. *Earth-Science Reviews*, 186:195—230.
- Wang, Y.J., Zhang, A.M., Cawood, P.A., et al., 2013. Geochronological, Geochemical and Nd-Hf-Os Isotopic Fingerprinting of an Early Neoproterozoic Arc-back-Arc System in South China and Its Accretionary Assembly along the Margin of Rodinia. *Precambrian Research*, 231:343—371. <https://doi.org/10.1016/j.precamres.2013.03.020>
- Wang, Y.J., Zhang, A.M., Fan, W.M., et al., 2010. Petrogenesis of Late Triassic Post-Collisional Basaltic Rocks of the Lancangjiang Tectonic Zone, Southwest China, and Tectonic Implications for the Evolution of the Eastern Paleotethys: Geochronological and Geochemical Constraints. *Lithos*, 120(3—4):529—546. <https://doi.org/10.1016/j.lithos.2010.09.012>
- Wang, X.F., Ma, D.Q., Jiang, D.H., 1991. Geology of Hainan Island: Structural Geology. Geological Publishing House, Beijing, 10—100 (in Chinese).
- Wen, S.N., Liang, X.Q., Fan, W.M., et al., 2013. Zircon U-Pb Ages, Hf Isotopic Composition of Zhizhong Granitic Intrusion in Ledong Area of Hainan Island and Their Tectonic Implications. *Geotectonica et Metallogenesis*, 37(2):294—307 (in Chinese with English abstract).
- Whalen, J.B., Currie, K.L., Chappell, B.W., 1987. A-Type Granites: Geochemical Characteristics, Discrimination and Petrogenesis. *Contributions to Mineralogy and Petrology*, 95(4):407—419. <https://doi.org/10.1007/bf0042202>
- Wright, J.B., 1969. A Simple Alkalinity Ratio and Its Application to Questions of Non-Orogenic Granite Genesis. *Geological Magazine*, 106(4):370. <https://doi.org/10.1017/s0016756800058222>
- Xia, X.P., Sun, M., Zhao, G.C., et al., 2004. Spot Zircon U-Pb Isotope Analysis by ICP-MS Coupled with a Frequency Quintupled (213 nm) Nd-YAG Laser System. *Geochemical Journal*, 38(2):191—200. <https://doi.org/10.2343/geochemj.38.191>
- Xia, B.D., Shi, G.Y., Fang, Z., et al., 1991. The Late Palaeozoic Rifting in Hainan Island, China. *Acta Geologica Sinica*, 65(2):103—115 (in Chinese with English abstract).
- Xia, B.D., Yu, J.H., Fang, Z., et al., 1990. Geochemical Characteristics and Origin of the Hercynian-Indosinian Granites of Hainan Island, China. *Geochimica*, 19(4):365—373 (in Chinese with English abstract).
- Xie, C.F., Zhu, J.C., Zhao, Z.J., et al., 2005. Zircon SHRIMP U-Pb Age Dating of Garnet-Acmite Syenite: Constraints on the Hercynian-Indosinian Tectonic Evolution of Hainan Island. *Geological Journal of China Universities*, 11(1):47—57 (in Chinese with English abstract).
- Yang, J.H., Wu, F.Y., Chung, S.L., et al., 2006. A Hybrid Origin for the Qianshan A-Type Granite, Northeast China: Geochemical and Sr-Nd-Hf Isotopic Evidence. *Lithos*, 89(1—2):89—106. <https://doi.org/10.1016/j.lithos.2005.10.002>
- Zen, E.A., 1986. Aluminum Enrichment in Silicate Melts by Fractional Crystallization: Some Mineralogic and Petrographic Constraints. *Journal of Petrology*, 27(5):1095—1117. <https://doi.org/10.1093/petrology/27.5.1095>
- Zhang, F.F., Wang, Y.J., Chen, X.Y., et al., 2011. Triassic High-Strain Shear Zones in Hainan Island (South China) and Their Implications on the Amalgamation of the Indochina and South China Blocks: Kinematic and ⁴⁰Ar/³⁹Ar Geochronological Constraints. *Gondwana Research*, 19(4):910—925. <https://doi.org/10.1016/j.gr.2010.11.002>
- Zhong, C.T., Deng, J.F., Wan, Y.S., et al., 2007. Magma Recording of Paleoproterozoic Orogeny in Central Segment of Northern Margin of North China Craton: Geochemical Characteristics and Zircon SHRIMP Dating of S-Type Granitoids. *Geochimica*, 36(6):585—600 (in Chinese with English abstract).
- Zhou, Z.M., Xie, C.F., Xu, Q., et al., 2011. Geological and Geochemical Characteristics of Middle Triassic Syenite-Granite Suite in Hainan Island and Its Geotectonic Implications. *Geological Review*, 57(4):515—531 (in Chinese with English abstract).
- Zi, J.W., Cawood, P.A., Fan, W.M., et al., 2012. Generation of Early Indosinian Enriched Mantle-Derived Granitoid Pluton in the Sanjiang Orogen (SW China) in Response to Closure of the Paleo-Tethys. *Lithos*, 140—141:166—182. <https://doi.org/10.1016/j.lithos.2012.02.006>

附中文参考文献

- 陈新跃,王岳军,范蔚茗,等,2011.海南五指山地区花岗片麻岩锆石LA-ICP-MS U-Pb年代学特征及其地质意义. *地球化学*, 40(5):454—463.
- 陈新跃,王岳军,韩会平,等,2014.琼西南三叠纪基性岩脉年代学、地球化学特征及其构造意义. *吉林大学学报(地球科学版)*, 44(3):835—847.

- 陈新跃,王岳军,韦牧,等,2006.海南公爱 NW 向韧性剪切带构造特征及其⁴⁰Ar-³⁹Ar 年代学约束.大地构造与成矿学,30(3):312—319.
- 广东省地质矿产局,1988.广东省区域地质志.北京:地质出版社.
- 胡宁,张仁杰,冯少南,2002.海南岛泥盆—石炭系界线研究.地质科学,37(3):313—319,387.
- 李孙雄,云平,范渊,等,2005.海南岛琼中地区琼中岩体锆石 U-Pb 年龄及其地质意义.大地构造与成矿学,29(2):227—233,241.
- 李献华,周汉文,丁式江,等,2000.海南岛洋中脊型变质基性岩:古特提斯洋壳的残片?科学通报,45(1):84—89.
- 刘颖,刘海臣,李献华,1996.用 ICP-MS 准确定测岩石样品中的 40 余种微量元素.地球化学,25(6):552—558.
- 龙文国,符策锐,朱耀河,2002.海南岛东部黄竹岭地区“抱板群”的解体.地层学杂志,26(3):212—215.
- 龙文国,童金南,朱耀河,等,2007.海南儋州—屯昌地区二叠纪地层的发现及其意义.华南地质与矿产,23(1):38—45.
- 马大铨,黄香定,肖志发,等,1998.海南岛结晶基底—抱板群层序与时代.武汉:中国地质大学出版,1—52.
- 沈宝云,刘兵,刘海龄,等,2016.海南岛小妹韧性剪切带的纳米尺度.地球科学,41(9):1489—1498.
- 唐立梅,2010.海南岛中生代两期构造伸展作用的岩浆记录及其大陆动力学意义(博士学位论文).杭州:浙江大学.
- 唐立梅,陈汉林,董传万,等,2013.海南岛中三叠世造山后伸展作用:双峰式侵入岩的年代学及地球化学制约.中国科学:地球科学,43(3):433—445.
- 汪啸风,马大铨,蒋大海,1991.海南岛地质(三)——构造地质.北京:地质出版社,10—100.
- 温淑女,梁新权,范蔚茗,等,2013.海南岛乐东地区志仲岩体锆石 U-Pb 年代学、Hf 同位素研究及其构造意义.大地构造与成矿学,37(2):294—307.
- 夏邦栋,施光宇,方中,等,1991.海南岛晚古生代裂谷作用.地质学报,65(2):103—115.
- 夏邦栋,于津海,方中,等,1990.海南岛海西—印支期花岗岩的地球化学特征及成因.地球化学,19(4):365—373.
- 谢才富,朱金初,赵子杰,等,2005.三亚石榴霓辉石正长岩的锆石 SHRIMP U-Pb 年龄:对海南岛海西—印支期构造演化的制约.高校地质学报,11(1):47—57.
- 钟长汀,邓晋福,万渝生,等,2007.华北克拉通北缘中段古元古代造山作用的岩浆记录:S 型花岗岩地球化学特征及锆石 SHRIMP 年龄.地球化学,36(6):585—600.
- 周佐民,谢才富,徐倩,等,2011.海南岛中三叠世正长岩—花岗岩套的地质地球化学特征与构造意义.地质论评,57(4):515—531.